Supporting Information

A Universal Strategy for Single-Atom Synthesis by Conductive Polymer-Modified Metal-Organic Frameworks Towards Enhanced Photocatalysis

*Yuting Zhu[a], Na Song[a], Shengjun Liu[*a], Kui Zhang[*a], Bo Liu[b] and Yang Wang[*c]*

Y. T. Zhu, N. Song, S. J. Liu, K. Zhang

School of Chemistry and Chemical Engineering, Anhui University of Technology, Ma'anshan, Anhui, 243032, P. R. China

E-mail: lsj1990@mail.ustc.edu.cn; zhangkui@mail.ustc.edu.cn

B. Liu

School of Chemistry and Materials Science, University of Science and Technology of China, Hefei, Anhui, 230026, P. R. China

Y. Wang

Department of Environmental Science and Engineering, University of Science and Technology of China, Hefei 230026, P. R. China

E-mail: ywangese@ustc.edu.cn

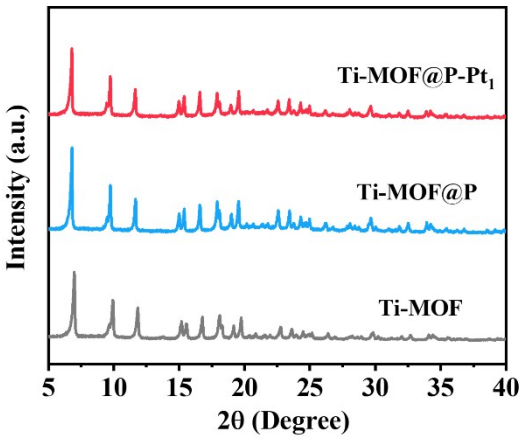

Figure S1. Powder XRD patterns of Ti-MOF, Ti-MOF@P and Ti-MOF@P-Pt_1.

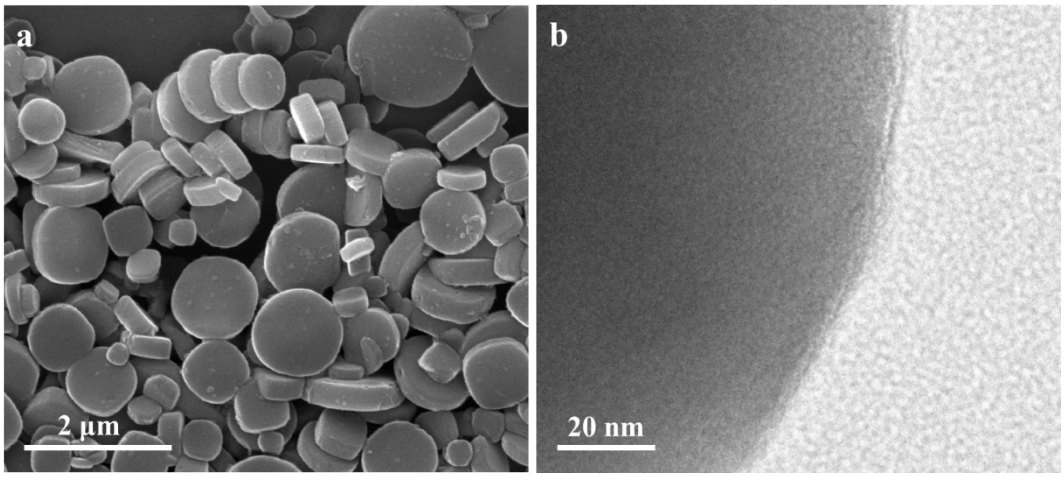

Figure S2. (a) SEM and (b) TEM images of Ti-MOF.

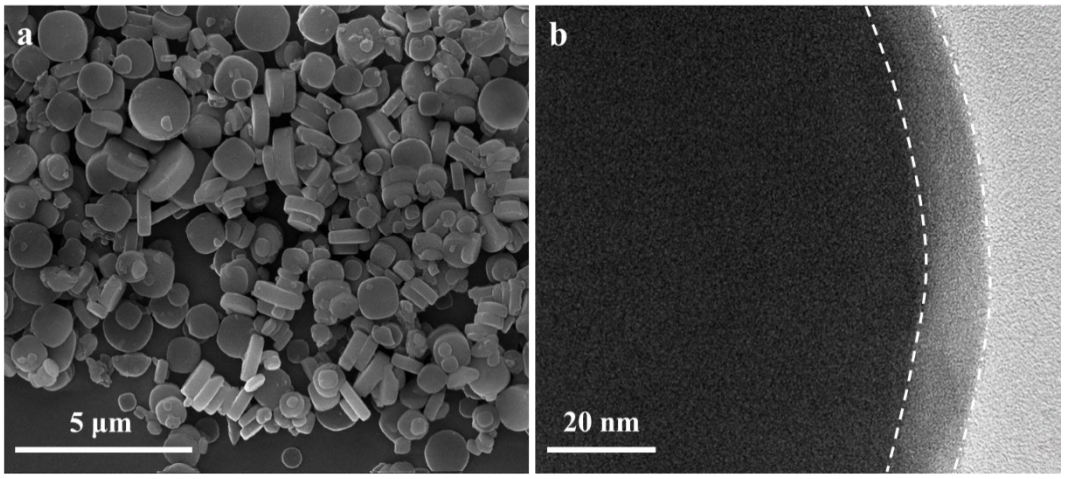

Figure S3. (a) SEM and (b) TEM images of Ti-MOF@P.

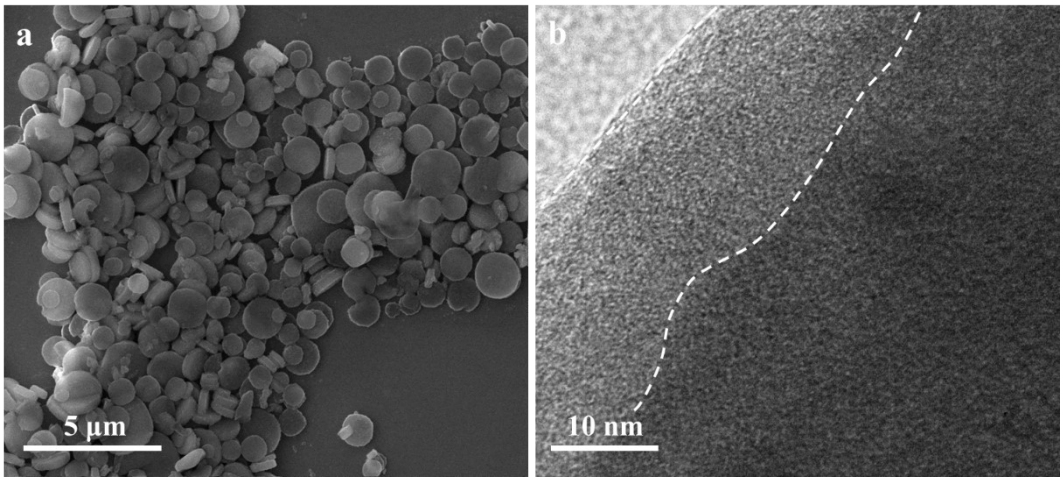

Figure S4. (a) SEM and (b) TEM images of Ti-MOF@P-Pt_1.

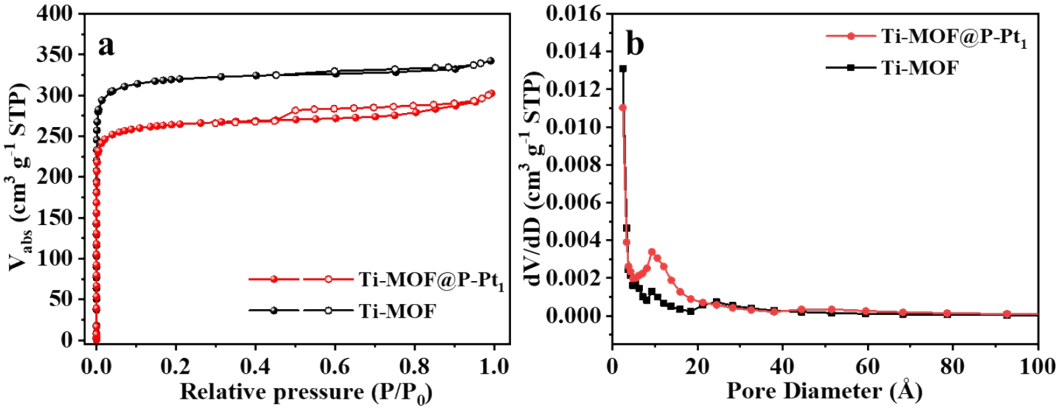

Figure S5. (a) N_2 sorption isotherms (solid: adsorption curve; open: desorption curve) and (b) pore size distribution on DFT method for Ti-MOF and Ti-MOF@P-Pt_1 at 77 K.

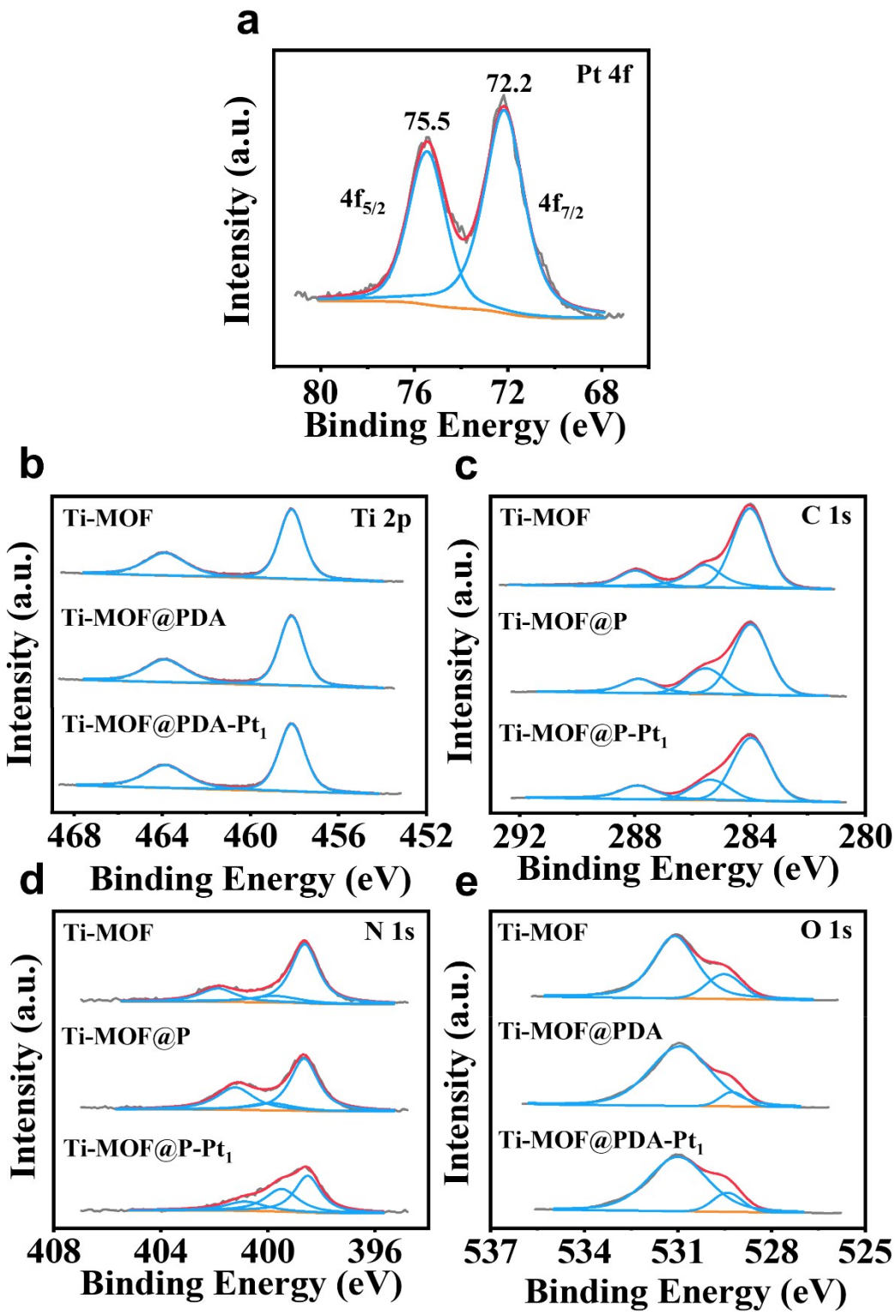

Figure S6. High-resolution XPS spectra of (a) Pt 4f in Ti-MOF@P-Pt_1, (b, c, d, e) Ti 2p, C 1s, N 1s and O 1s in Ti-MOF, Ti-MOF@P, Ti-MOF@P-Pt_1.

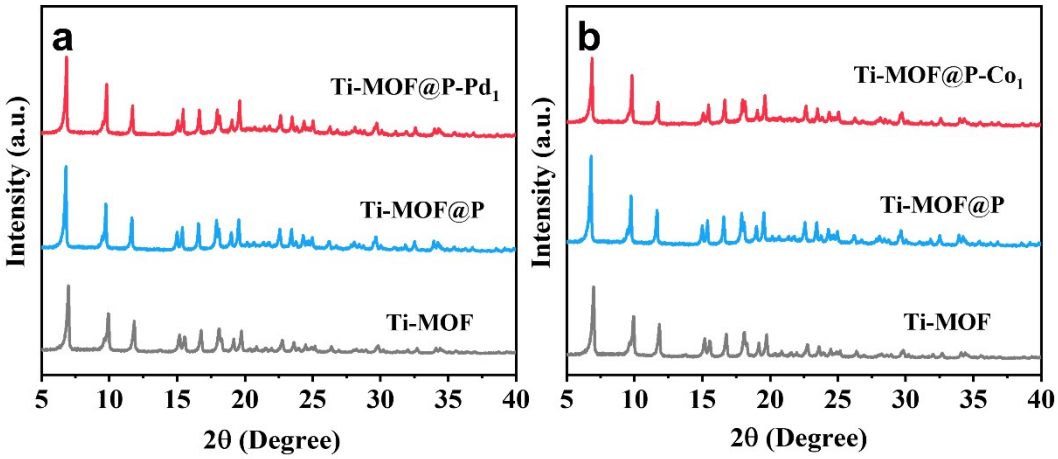

Figure S7. Powder XRD patterns of (a) Ti-MOF, Ti-MOF@P, and Ti-MOF@P-Pd_1 and (b)Ti-MOF, Ti-MOF@P, and Ti-MOF@P-Co_1.

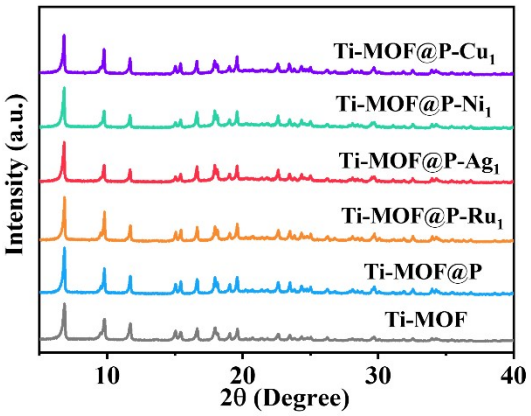

Figure S8. Powder XRD patterns of (a) Ti-MOF, as well as Ti-MOF@P, Ti-MOF@P-M_1.

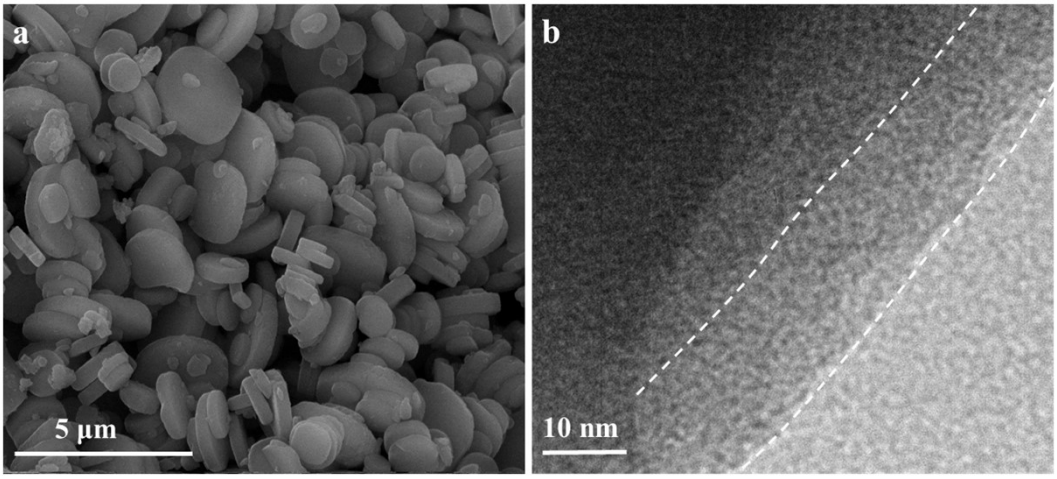

Figure S9. (a) SEM and (b) HRTEM image of Ti-MOF@P-Pd_1.

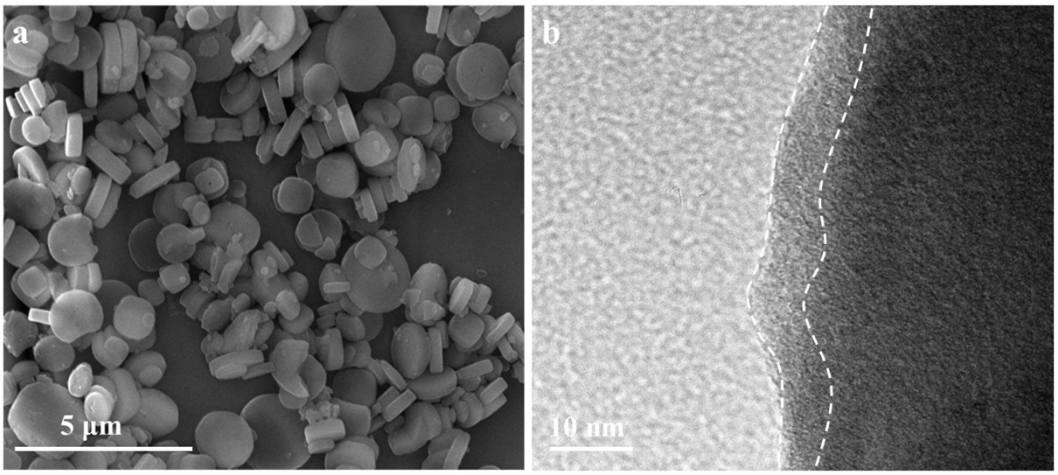

Figure S10. (a) SEM and (b) HRTEM images of Ti-MOF@P-Co_1.

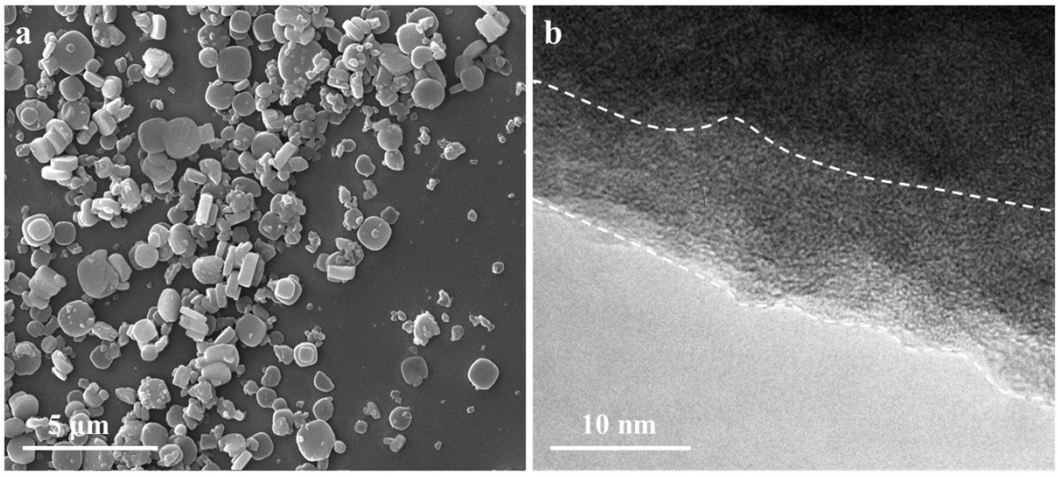

Figure S11. (a) SEM and (b) HRTEM images of Ti-MOF@P-Ru_1.

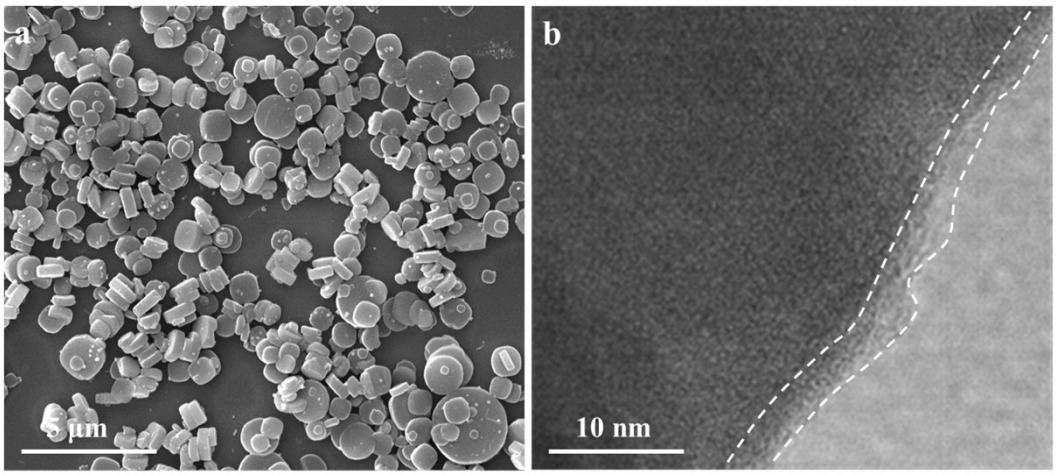

Figure S12. (a) SEM and (b) HRTEM images of Ti-MOF@P-Ag_1.

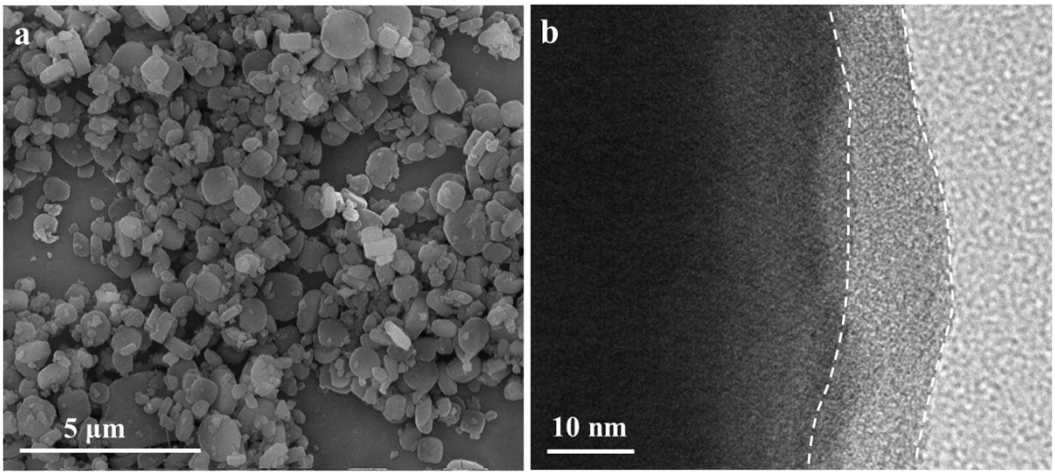

Figure S13. (a) SEM and (b) HRTEM images of Ti-MOF@P-Ni_1.

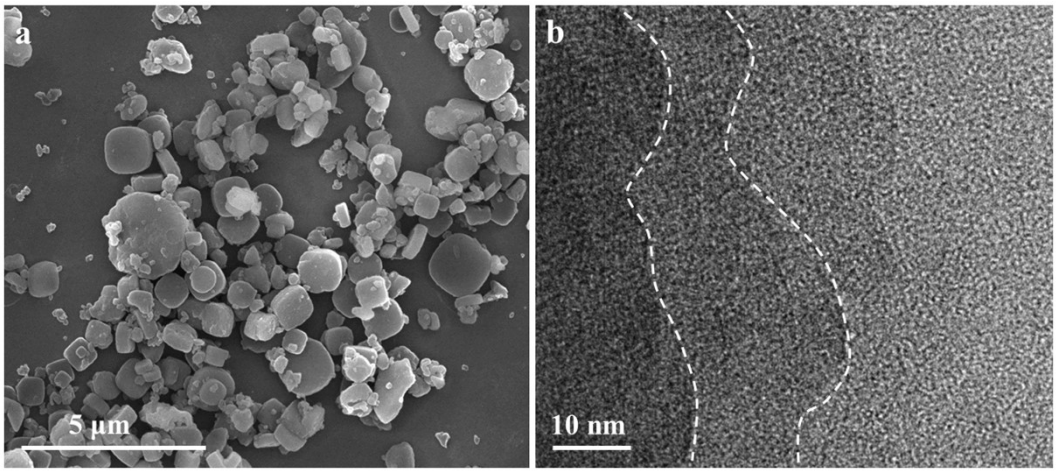

Figure S14. (a) SEM and (b) HRTEM images of Ti-MOF@P-Cu_1.

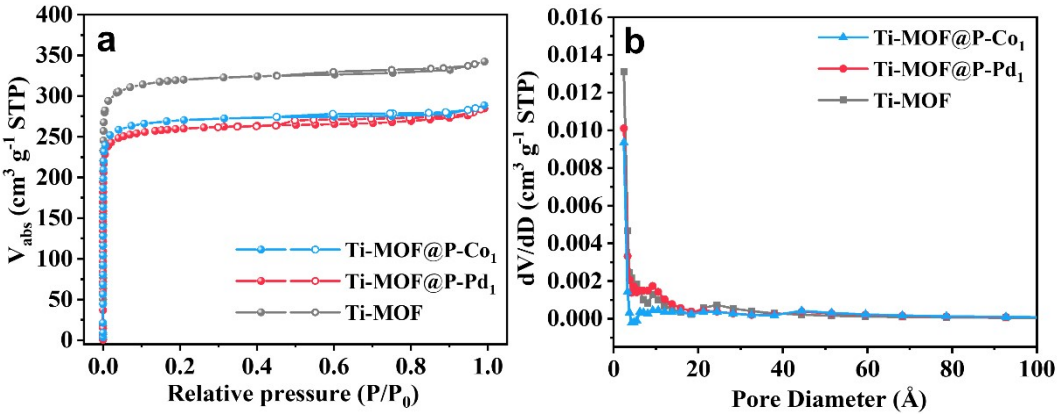

Figure S15. (a) N_2 sorption isotherms (solid: adsorption curve; open: desorption curve) and (b) pore size distribution on DFT method for Ti-MOF, Ti-MOF@P-Pd_1 and Ti-MOF@P-Co_1 at 77 K.

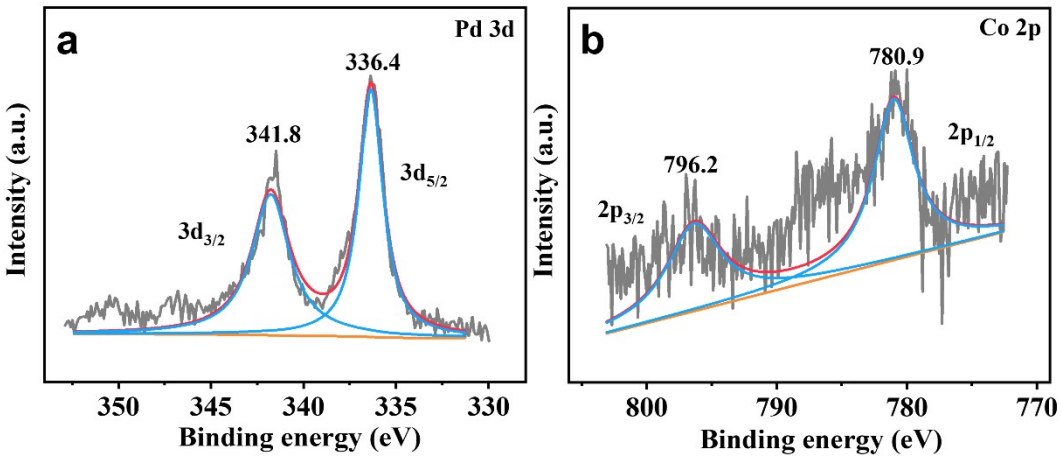

Figure S16. (a) High-resolution XPS spectrum of Pd 3d in Ti-MOF@P-Pd_1. (b) High-resolution XPS spectrum of Co 2p in Ti-MOF@P-Co_1.

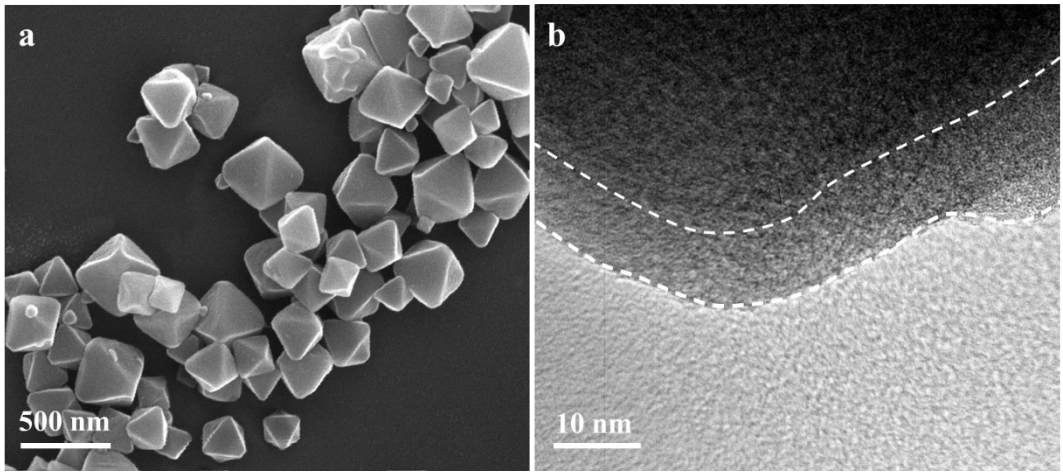

Figure S17. (a) TEM and (b) HRTEM images of NH_2-UiO-66@P-Pt_1.

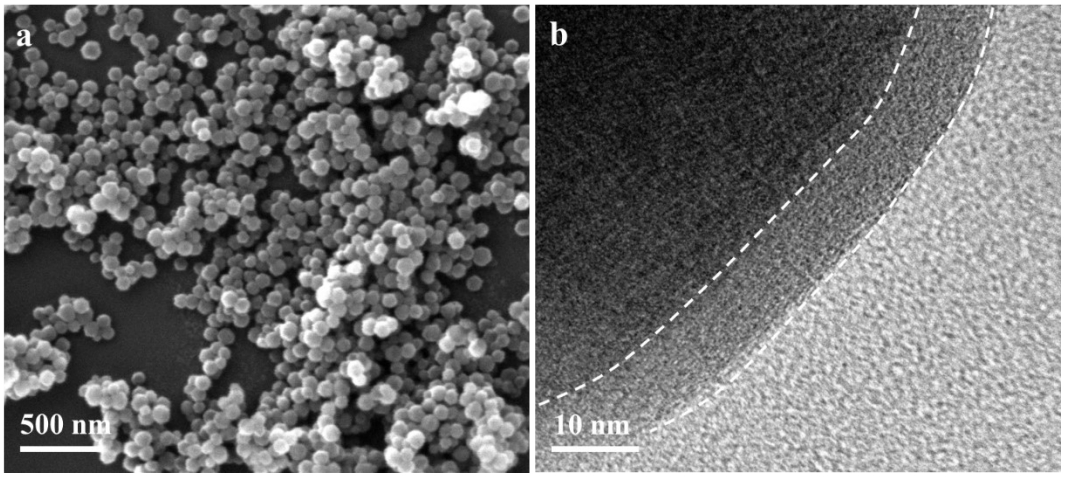

Figure S18. (a) TEM and (b) HRTEM images of MOF-808@P-Pt_1.

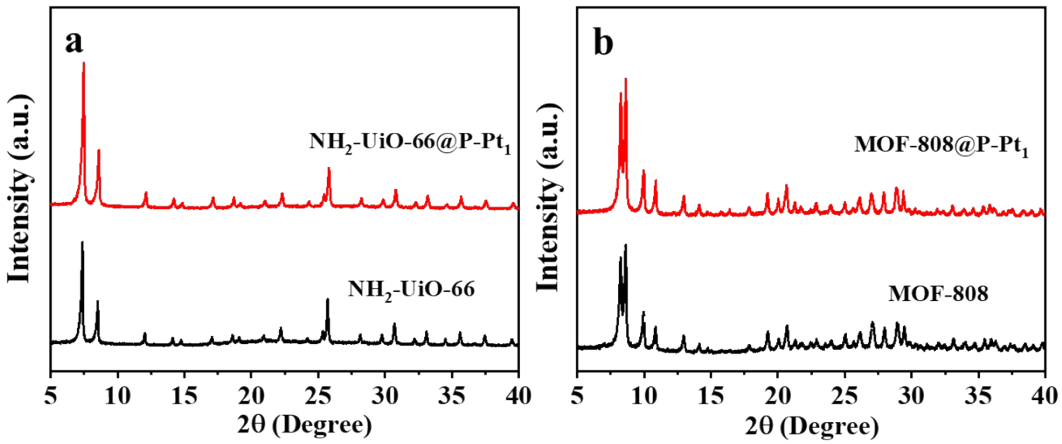

Figure S19. Powder XRD patterns of (a) NH_2-UiO-66, NH_2-UiO-66@P and NH_2-UiO-66@P-Pt_1 and (b) MOF-808, MOF-808@P and MOF-808@P-Pt_1.

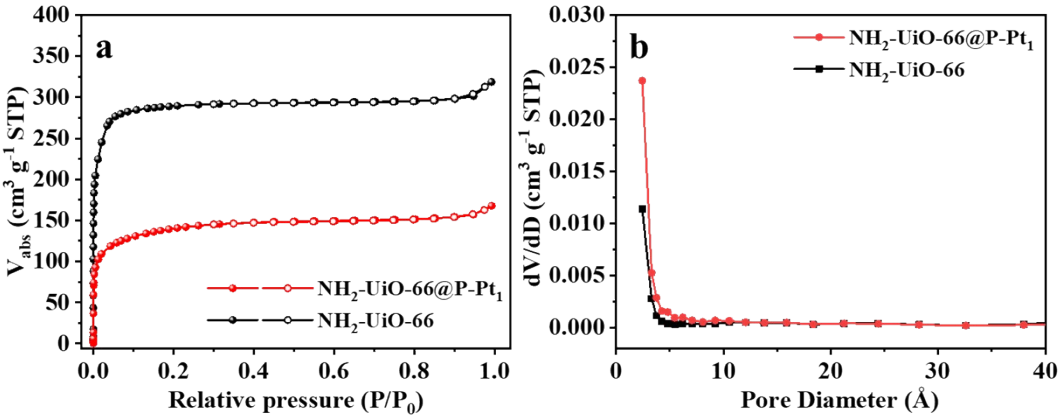

Figure S20. (a) N_2 sorption isotherms and (b) pore size distribution on DFT method for NH_2-UiO-66 and NH_2-UiO-66@P-Pt_1.

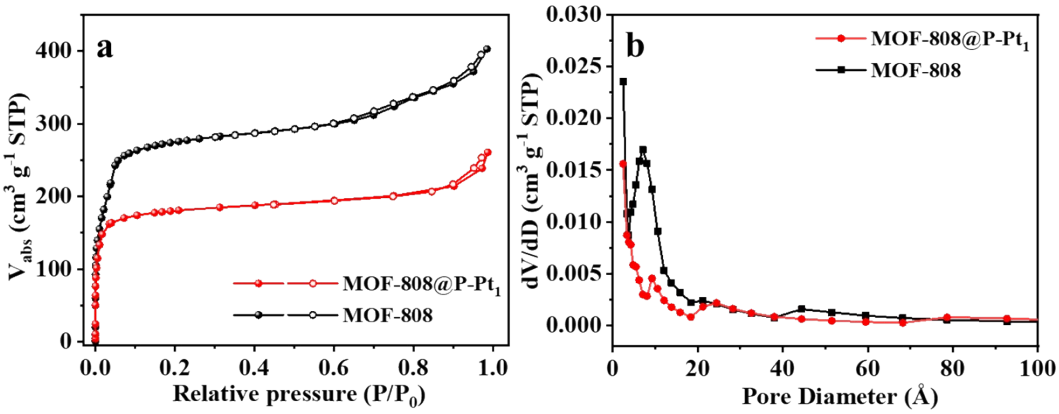

Figure S21. (a) N_2 sorption isotherms and (b) pore size distribution on DFT method for MOF-808 and MOF-808@P-Pt_1.

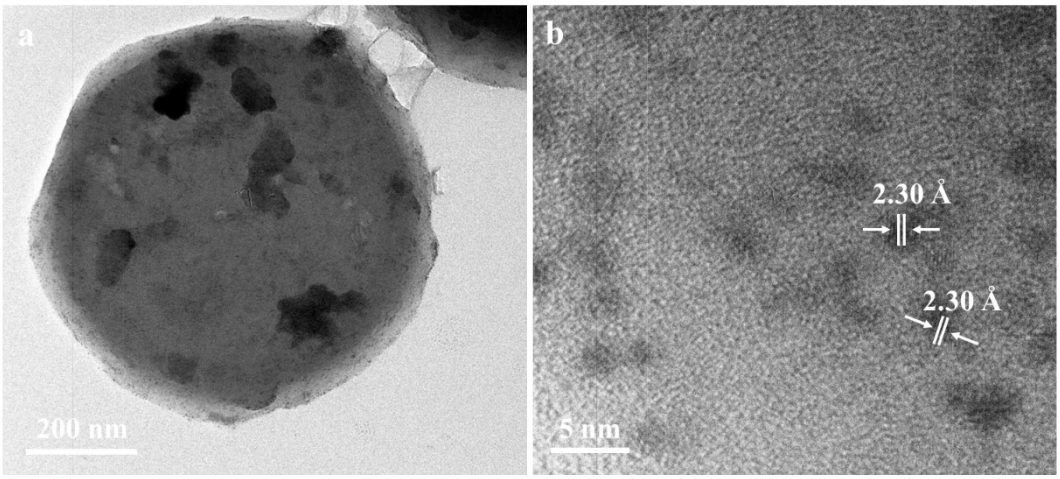

Figure S22. TEM and HRTEM image of Ti-MOF@P-Pt_{NP}.

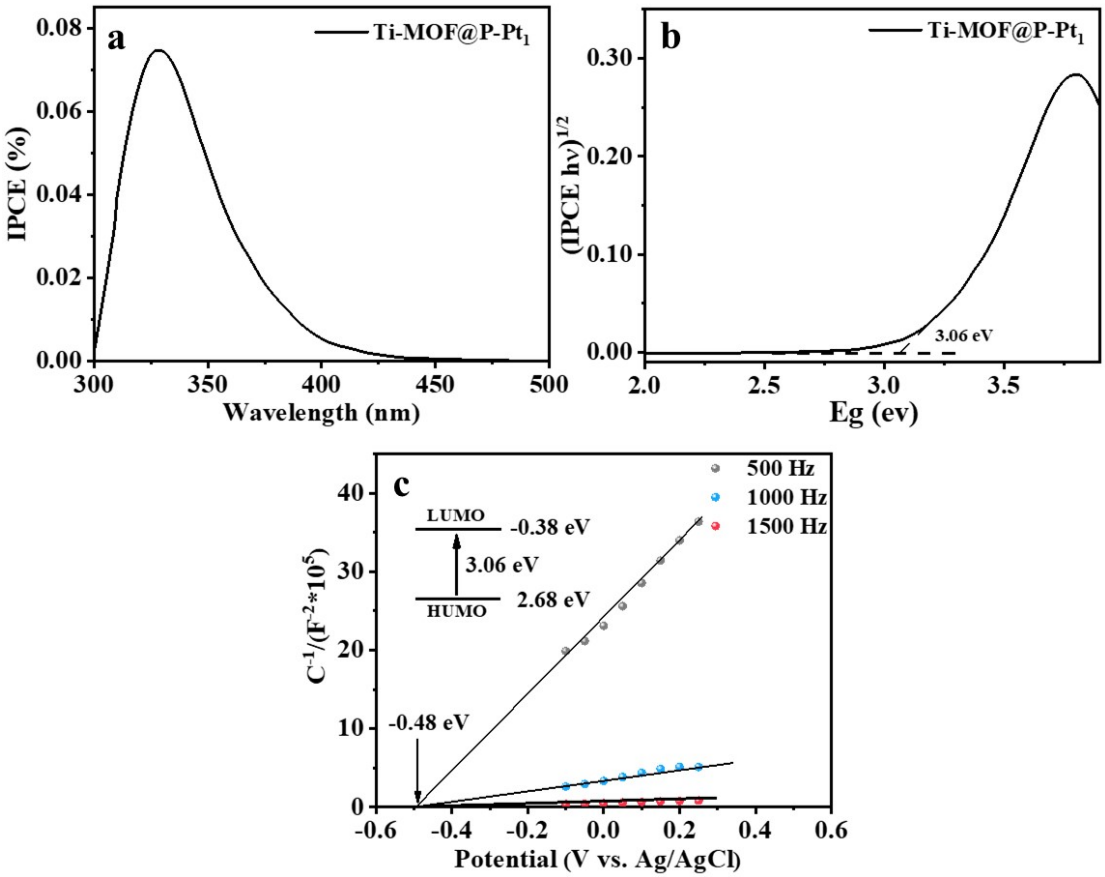

Figure S23. (a) IPCE spectra, (b) Band gap energy determined from the (IPCE hν)$^{1/2}$ vs. hν curve and (c) Mott-Schottky plots of Ti-MOF@P-Pt$_1$. (Inset: the energy diagram of Ti-MOF@P-Pt$_1$).

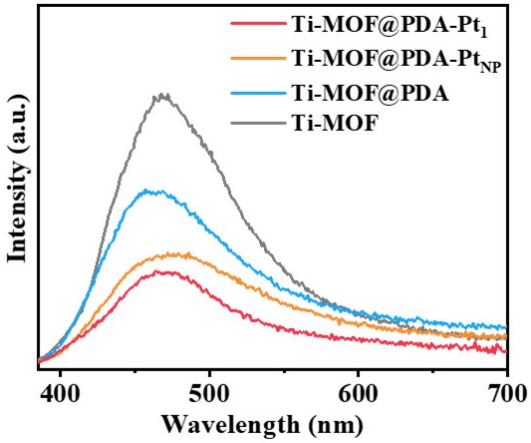

Figure S24. PL emission spectra (λ_{ex} = 365 nm) of Ti-MOF, Ti-MOF@P, Ti-MOF@P-Pt_{NP}, Ti-MOF@P-Pt_1.

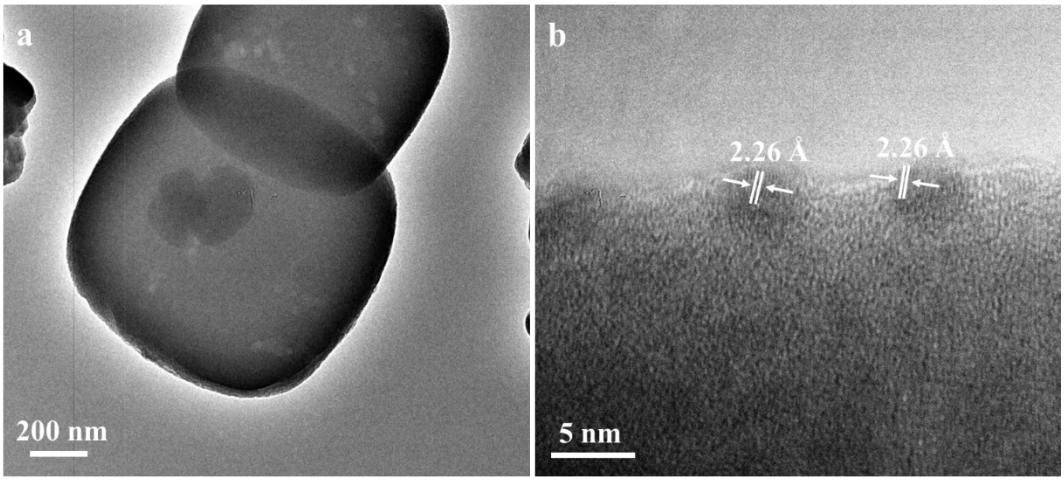

Figure S25. (a) TEM and (b) HRTEM images of Ti-MOF@P-Pd_{NP}.

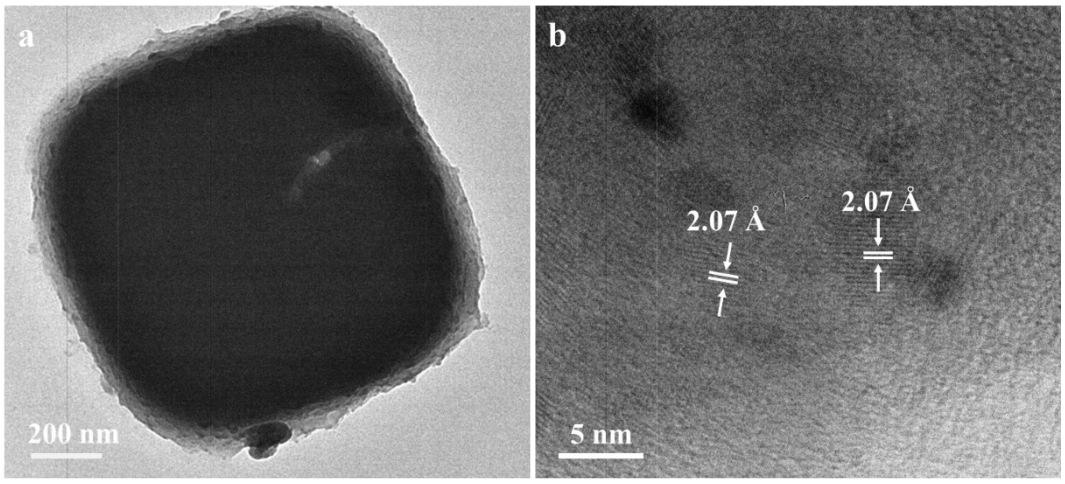

Figure S26. (a) TEM and (b) HRTEM images of Ti-MOF@P-Co_{NP}.

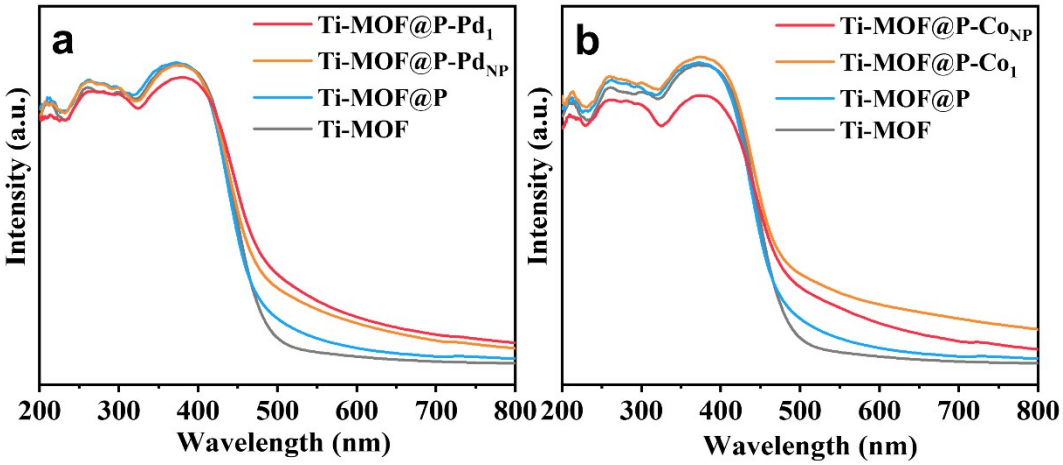

Figure S27. UV-vis diffuse reflectance spectra for (a) Ti-MOF, Ti-MOF@P, Ti-MOF@P-Pd_{NP} and Ti-MOF@P-Pd_1, and (b) Ti-MOF, Ti-MOF@P, Ti-MOF@P-Co_{NP} and Ti-MOF@P-Co_1.

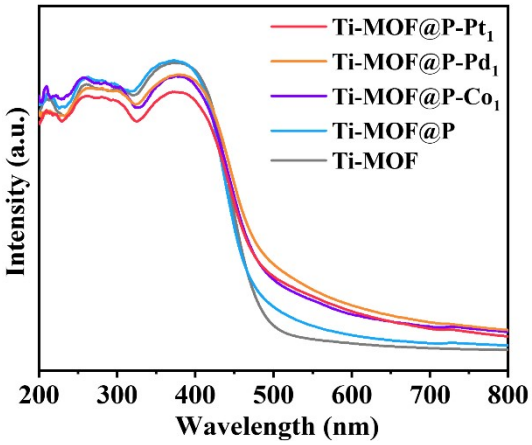

Figure S28. UV-vis diffuse reflectance spectra for Ti-MOF, Ti-MOF@P, Ti-MOF@P-Co_1, Ti-MOF@P-Pd_1 and Ti-MOF@P-Pt_1.

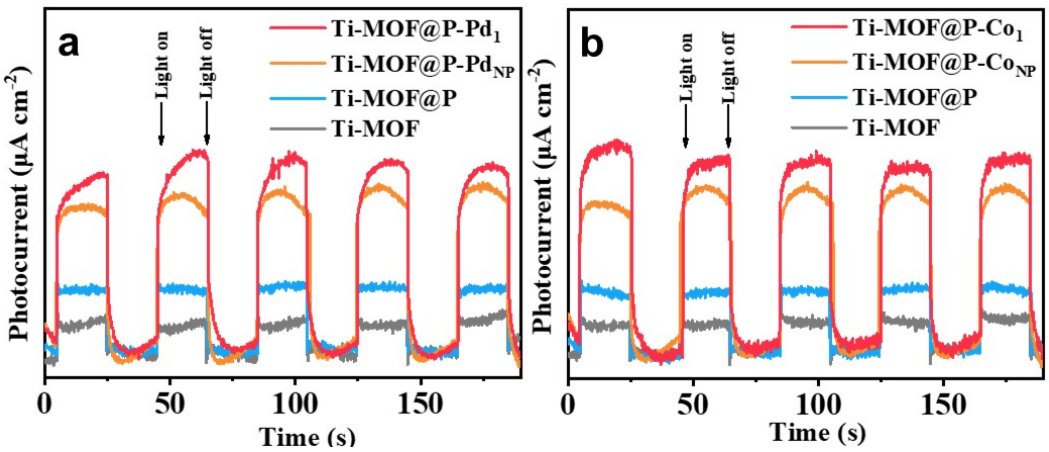

Figure S29. Photocurrent responses for (a) Ti-MOF, Ti-MOF@P, Ti-MOF@P-Pd_{NP} and Ti-MOF@P-Pd_1, and (b) Ti-MOF, Ti-MOF@P, Ti-MOF@P-Co_{NP} and Ti-MOF@P-Co_1.

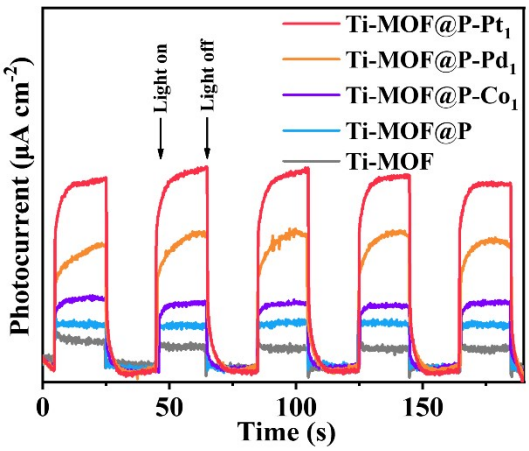

Figure S30. Photocurrent responses for Ti-MOF@P, Ti-MOF@P, Ti-MOF@P-Co_1, Ti-MOF@P-Pd_1 and Ti-MOF@P-Pt_1.

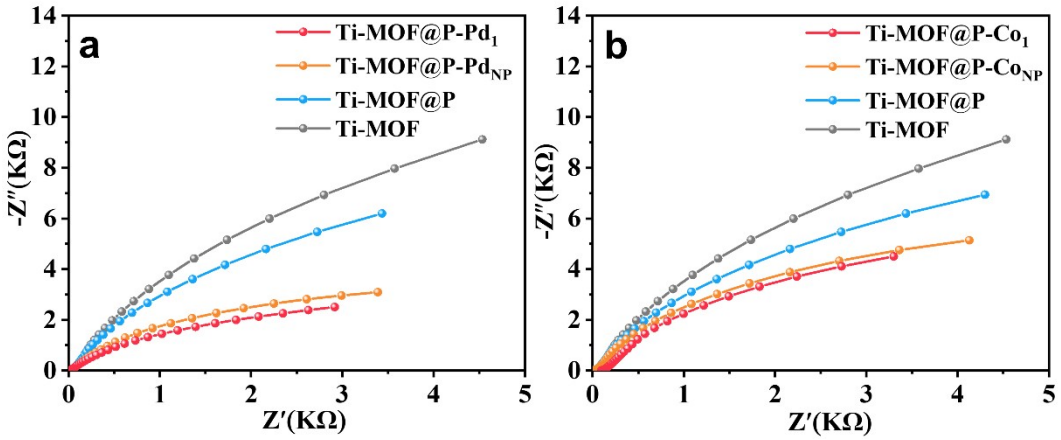

Figure S31. EIS Nyquist plots for (a) Ti-MOF, Ti-MOF@P, Ti-MOF@P-Pd_{NP} and Ti-MOF@P-Pd_1, and (b) Ti-MOF, Ti-MOF@P, Ti-MOF@P-Co_{NP} and Ti-MOF@P-Co_1.

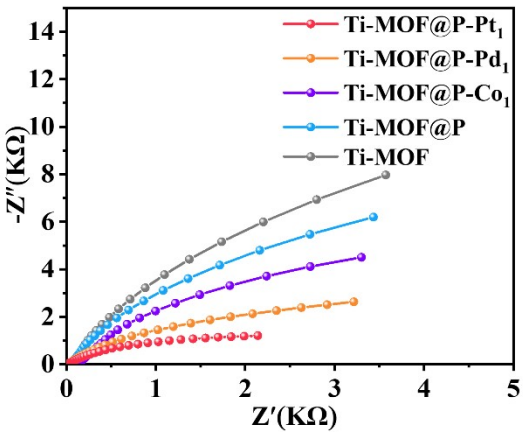

Figure S32. EIS Nyquist plots for Ti-MOF, Ti-MOF@P, Ti-MOF@P-Co_1, Ti-MOF@P-Pd_1 and Ti-MOF@P-Pt_1.

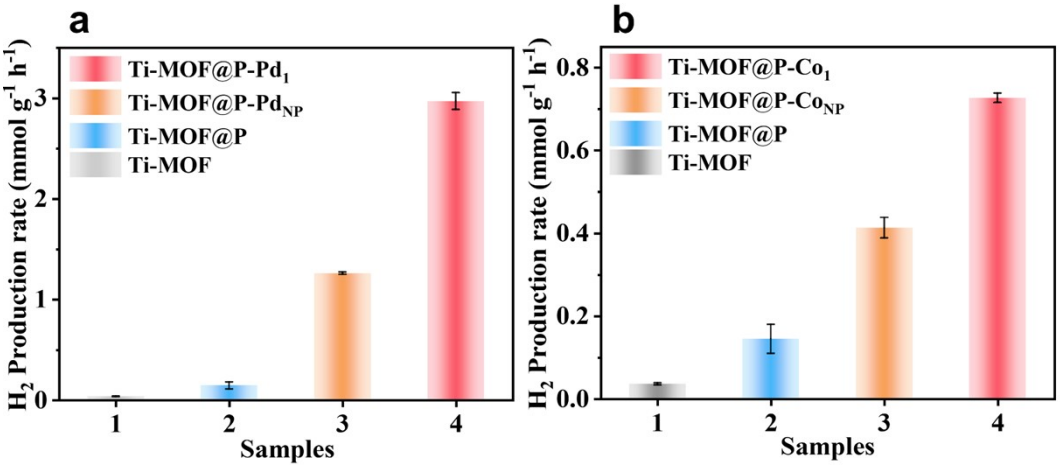

Figure S33. Photocatalytic hydrogen production rates for (a) Ti-MOF, Ti-MOF@P, Ti-MOF@P-Pd_{NP} and Ti-MOF@P-Pd_1, and (b) Ti-MOF, Ti-MOF@P, Ti-MOF@P-Co_{NP} and Ti-MOF@P-Co_1. Error bars represent the standard deviations of three independent measurements.

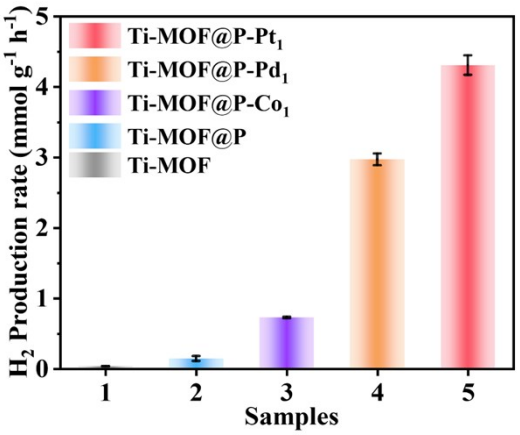

Figure S34. Photocatalytic hydrogen production rates for Ti-MOF, Ti-MOF@P, Ti-MOF@P-Co_1, Ti-MOF@P-Pd_1. Error bars represent the standard deviations of three independent measurements.

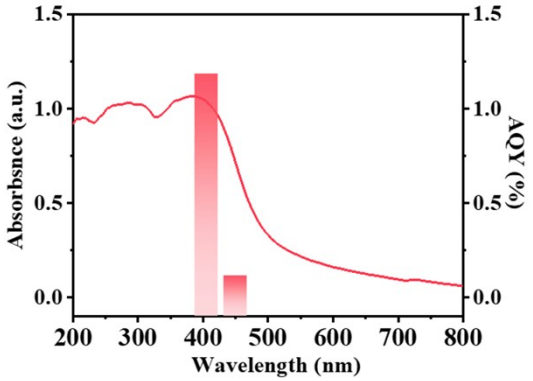

Figure S35. Apparent quantum efficiency test of Ti-MOF@P-Pt_1 samples under 405 nm and 450 nm wavelength illumination.

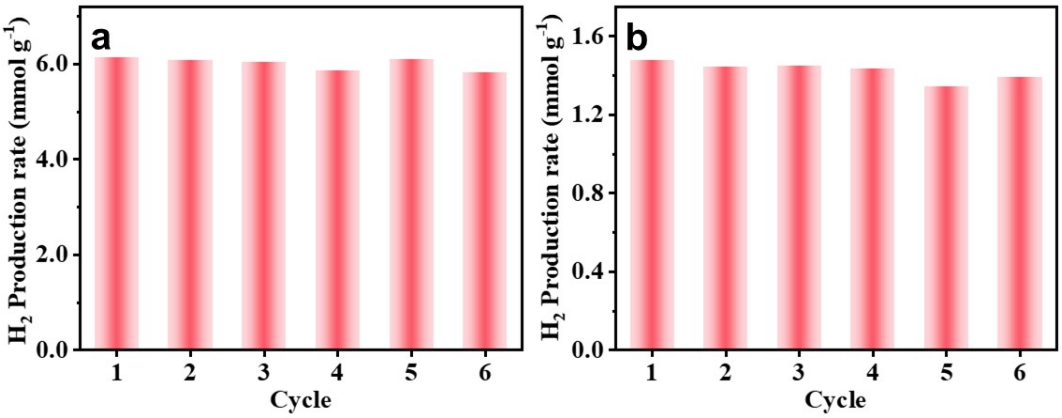

Figure S36. The consecutive 6 runs of photocatalytic recycling performance for (a) Ti-MOF@P-Pd_1 and (b) Ti-MOF@P-Co_1.

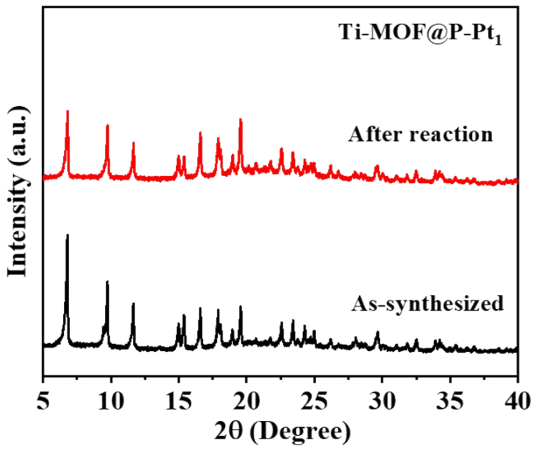

Figure S37. Powder XRD patterns of Ti-MOF@P-Pt_1 before and after photocatalytic reaction.

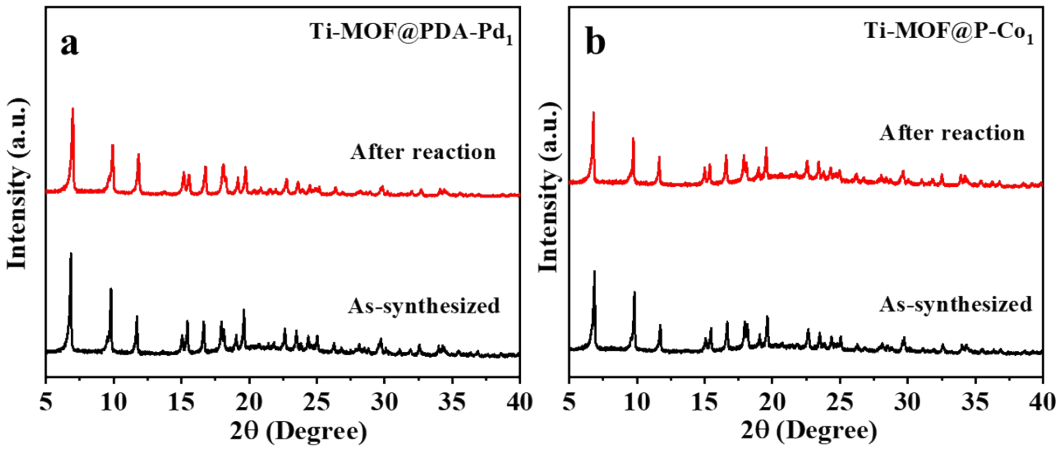

Figure S38. Powder XRD patterns of (a) Ti-MOF@P-Pd_1 before and after photocatalytic reaction, and (b) Ti-MOF@P-Co_1 before and after photocatalytic reaction.

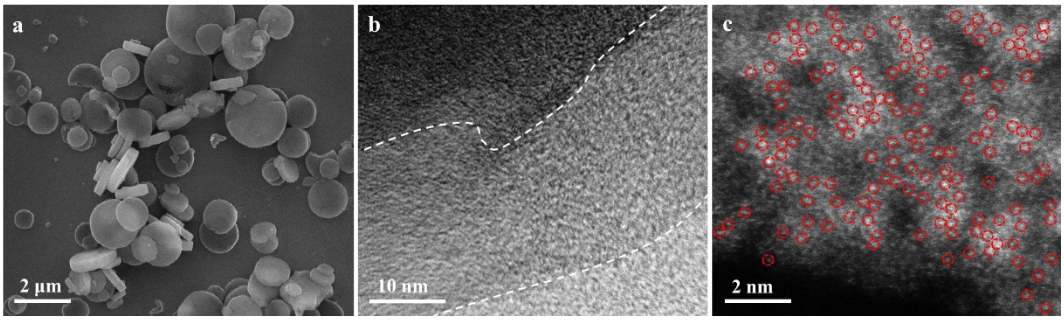

Figure S39. (a) SEM and (b) HRTEM and (c) HAADF-STEM images of Ti-MOF@P-Pt_1 after reaction.

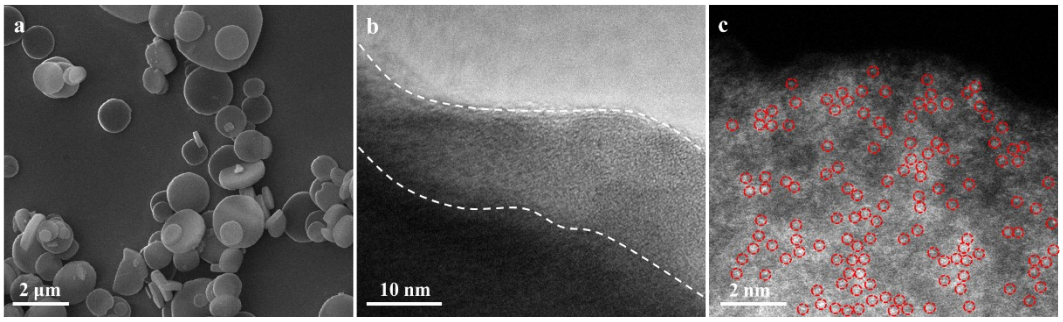

Figure S40. (a) SEM and (b) HRTEM and (c) HAADF-STEM images of Ti-MOF@P-Pd_1 after reaction.

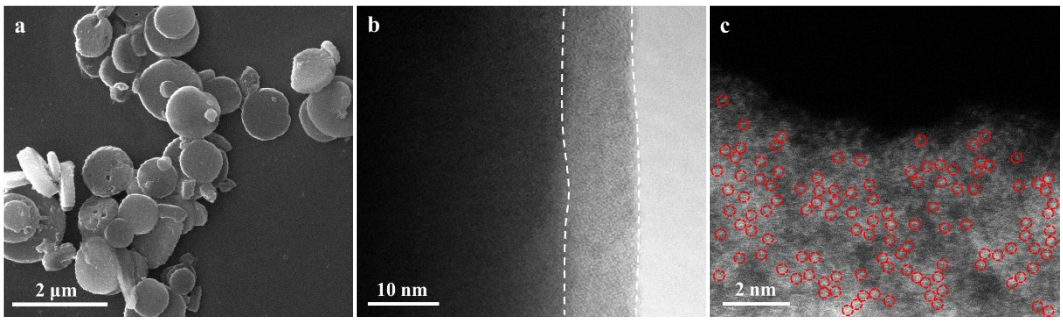

Figure S41. (a) SEM and (b) HRTEM and (c) HAADF-STEM images of Ti-MOF@P-Co_1 after reaction.

Table S1. EXAFS data fitting parameters and results for Ti-MOF@P-Pt_1.

Catalysts	Path	N	R(Å)	σ^2 (10^{-3}Å^2)	ΔE_0 (eV)	R factor
Ti-MOF@P-Pt_1	M-O	3.71	2.01	0.006	9.028	0.014
	M-N	1.43	3.03	0.001	9.028	0.014

Table S2. The fitted fluorescence decay components of Ti-MOF, Ti-MOF@P, and Ti-MOF@P-Pt_{NP}, Ti-MOF@P-Pt_1.

Catalysts	τ_1 /ns	A_1	τ_2 /ns	A_2	τ_3 /ns	A_3	τ_a /ns
Ti-MOF	0.21±0.01	34.71%	4.44±0.13	65.29%	-	-	2.97±0.13
Ti-MOF@P	1.31±0.04	33.99%	7.68±0.10	66.01%	-	-	5.52±0.10
Ti-MOF@P-Pt_{NP}	0.76±0.02	38.67%	4.90±0.37	36.22%	18.31±2.08	25.10%	6.67±1.04
Ti-MOF@P-Pt_1	0.44±0.01	28.03%	3.76±0.22	34.65%	20.64±1.56	37.32%	9.13±1.00

Table S3. Elemental contents determined by ICP-MS for Ti-MOF@P-M_1 and Ti-MOF@P-M_{NP}.

Catalysts	M_1 (wt.%)	Catalysts	M_{NP} (wt.%)
Ti-MOF@P-Pt_1	1.20%	Ti-MOF@P-Pt_{NP}	1.12%
Ti-MOF@P-Pd_1	0.09%	Ti-MOF@P-Pd_{NP}	0.11%
Ti-MOF@P-Co_1	0.93%	Ti-MOF@P-Co_{NP}	0.94%

Table S4. Comparison of the hydrogen production activity of Ti-MOF@P-Pt_1 with that of the reported MOF-based single-atom photocatalysts.

Catalysts	Single atom species	Amount of H_2	Ref.
Al-TCPP-0.1Pt	Pt	129 μmol g^{-1} h^{-1}	[1]
HNTM-Ir/Pt	Ir; Pt	201.9 μmol g^{-1} h^{-1}	[2]
Pd_{10}@Pt_1/UiO-66-NH_2	Pt	1200.5 μmol g^{-1} h^{-1}	[3]
Ni_1-S/MOF	Ni	1360 μmol g^{-1} h^{-1}	[4]
Pt_1/SnO_2/UiO-66-NH_2	Pt	2167 μmol g^{-1} h^{-1}	[5]
Pt@UiO-66	Pt	3871.4 μmol g^{-1} h^{-1}	[6]
Ru_1/UiO-67-m-$(NH_2)_2$	Ru	4470 μmol g^{-1} h^{-1}	[7]
Pt-MOF	Pt	6640 μmol g^{-1} h^{-1}	[8]
Ti-MOF@P-Pt_1	Pt	4193 μmol g^{-1} h^{-1}	This work

References

1 X. Fang, Q. Shang, Y. Wang, L. Jiao, T. Yao, Y. Li, Q. Zhang, Y. Luo, H.-L. Jiang, *Adv. Mater.*, 2018, **30**, 1705112.

2 T. He, S. Chen, B. Ni, Y. Gong, Z. Wu, L. Song, L. Gu,W. Hu, X. Wang, *Angew. Chem., Int. Ed.*, 2018, **130**, 3551-3556.

3 Y. Pan, Y. Qian, X. Zheng, S. Chu, Y. Yang, C. Ding, X. Wang, S. Yu, H.-L. Jiang, *Nat. Sci. Rev.*, 2021, **8**, nwaa224.

4 X. Ma, H. Liu, W. Yang, G. Mao, L. Zheng, H.-L. Jiang, *J. Am. Chem. Soc.*, 2021, **143**, 12220-12229.

5 J. Sui, H. Liu, S. Hu, K. Sun, G. Wan, H. Zhou, X. Zheng, H.-L. Jiang, *Adv. Mater.*, 2022, **34**, 2109203.

6 Y. Zhang, P. Yan, Y. Zhou, Q. Xu, *Phys. Chem. Chem. Phys.*, 2022, **24**, 27515-27523.

7 S. Hu, M.-L. Gao, J. Huang, H. Wang, Q. Wang, W. Yang, Z. Sun, X. Zheng, H.-L. Jiang, *J. Am. Chem. Soc.*, 2024, **146**, 20391-20400.

8 J. H. Kim, Dr. S. Wu, Dr. L. Zdrazil, N. Denisov, Prof. P. Schmuki, *Angew. Chem., Int. Ed.*,2024, **63**, e202319255.